Novel detector design for reducing intercell x-ray cross-talk in the variable resolution x-ray CT scanner: A Monte Carlo study

Hosein Arabi and Ali Reza Kamali Asl[a)]
Department of Radiation Medicine, Shahid Beheshti University, 1983963113 Tehran, Iran

Mohammad Reza Ay
Research Centre for Science and Technology in Medicine, Tehran University of Medical Sciences, 1417613151 Tehran, Iran; Department of Medical Physics and Biomedical Engineering, Tehran University of Medical Sciences, 1417613151 Tehran, Iran; and Research Institute for Nuclear Medicine, Tehran University of Medical Sciences, 1417613151 Tehran, Iran

Habib Zaidi
Division of Nuclear Medicine, Geneva University Hospital, CH-1211 Geneva, Switzerland; Geneva Neuroscience Center, Geneva University, CH-1211 Geneva, Switzerland; and Department of Nuclear Medicine and Molecular Imaging, University Medical Center Groningen, University of Groningen, 9700 RB Groningen, Netherlands

(Received 12 October 2010; revised 25 December 2010; accepted for publication 24 January 2011; published 17 February 2011)

Purpose: The variable resolution x-ray (VRX) CT scanner provides substantial improvement in the spatial resolution by matching the scanner's field of view (FOV) to the size of the object being imaged. Intercell x-ray cross-talk is one of the most important factors limiting the spatial resolution of the VRX detector. In this work, a new cell arrangement in the VRX detector is suggested to decrease the intercell x-ray cross-talk. The idea is to orient the detector cells toward the opening end of the detector.

Methods: Monte Carlo simulations were used for performance assessment of the oriented cell detector design. Previously published design parameters and simulation results of x-ray cross-talk for the VRX detector were used for model validation using the GATE Monte Carlo package. In the first step, the intercell x-ray cross-talk of the actual VRX detector model was calculated as a function of the FOV. The obtained results indicated an optimum cell orientation angle of 28° to minimize the x-ray cross-talk in the VRX detector. Thereafter, the intercell x-ray cross-talk in the oriented cell detector was modeled and quantified.

Results: The intercell x-ray cross-talk in the actual detector model was considerably high, reaching up to 12% at FOVs from 24 to 38 cm. The x-ray cross-talk in the oriented cell detector was less than 5% for all possible FOVs, except 40 cm (maximum FOV). The oriented cell detector could provide considerable decrease in the intercell x-ray cross-talk for the VRX detector, thus leading to significant improvement in the spatial resolution and reduction in the spatial resolution nonuniformity across the detector length.

Conclusions: The proposed oriented cell detector is the first dedicated detector design for the VRX CT scanners. Application of this concept to multislice and flat-panel VRX detectors would also result in higher spatial resolution. © *2011 American Association of Physicists in Medicine*.
[DOI: 10.1118/1.3555035]

Key words: variable resolution x-ray (VRX) CT, intercell cross-talk, Monte Carlo, detector, system design

I. INTRODUCTION

Computed tomography (CT) can provide diagnostic quality high resolution images of the human anatomy *in vivo*. These valuable features have made it a powerful tool in diagnostic imaging. Depending on the size of the object being imaged, CT scanners have different field of view (FOV) and spatial resolution. Clinical CT scanners have relatively large FOV (up to 50 cm) and moderate spatial resolution (2–3 cycles/mm) for whole body imaging.[1,2] Decreasing the object size has no effect on the resulting spatial resolution of clinical CT scanners. On the other hand, micro-CT scanners are appropriate for imaging small objects. Such scanners have spatial resolution of up to 100 cycles/mm; they are, however, limited by the corresponding small FOV.[2,3]

The newly introduced CT scanners, such as the variable resolution x-ray (VRX) CT, combine the advantages of both clinical and micro-CT scanners. This design provides the possibility to adjust the spatial resolution according to the object size.[4,5] The concept consists of decreasing the apparent cell's width in the object plane to improve the detector's spatial resolution through angulation of the detector with re-

spect to the incident x-ray beam. This technique provides substantial improvement in the detector's spatial resolution and by changing the detector angle with respect to the x-ray beam, variable resolution can be achieved.[6,7] The VRX CT scanner allows imaging the objects at the highest possible spatial resolution according to their size or FOV. Small objects are imaged at high spatial resolution and small FOV, whereas large objects are imaged at a corresponding FOV at the cost of a reduced spatial resolution.

The idea of angulating the detection system to improve the spatial resolution can be applied in a large variety of applications. In the single array VRX detector, the spatial resolution improvement is due to a decrease in the apparent cell's size in the *x-y* plane, while the axial spatial resolution remains unchanged. Flat-panel and cone-beam VRX CT scanners can improve the spatial resolution not only in the transaxial plane but also in the axial direction.[8,9] Multiarm VRX CT scanners have several detector arms that can acquire images at different spatial resolutions using a single scan.[10,11] Each of these CT scanners has its own limitations and requires specific calibration parameters that that need to be determined.[12–15]

The spatial resolution in the VRX detector is limited by several physical factors, intercell x-ray cross-talk being one of them for all variants of VRX CT detector designs.[16] The intercell x-ray cross-talk is defined as the percentage of radiation that can penetrate from one cell to the other cells through cell separators. X-ray attenuation of separators is one of the main factors that influence the intercell x-ray cross-talk. Therefore, x-ray cross-talk can be reduced by increasing x-ray attenuation. In VRX detectors, intercell x-ray cross-talk is of special importance because angulation of the detector changes the angle between the incident x-ray beam and the detector cells. The intercell x-ray cross-talk widens the detector line spread function (LSF) and as such reduces the detector spatial resolution.[17–19]

A brief qualitative description and quantitative analysis of x-ray cross-talk have been reported earlier.[4,16] The qualitative study presented a wide range of theoretical analysis without any specific model, whereas in the quantitative study, an actual VRX CT detector was simulated through Monte Carlo to investigate intercell and interarm x-ray cross-talk as a function of the size of the detector's FOV. The intercell x-ray cross-talk at FOVs of 24–38 cm was over the desirable value.[16] It was suggested to scan all objects between 24 and 40 cm in diameter with the 40 cm FOV to minimize the deteriorating effect of intercell x-ray cross-talk on the resulting spatial resolution of the system.

In this work, a novel VRX detector design (oriented cell detector) is proposed to reduce the intercell x-ray cross-talk. The idea is to orient the detector cells toward the opening end of the detector so that the detector cells and separators are parallel to the incident x-ray beam. The objectives of this study are to determine the optimum orientation angle for detector cells to minimize intercell x-ray cross-talk and to quantify its magnitude in the oriented cell detector. The achieved performance of the proposed design in terms of intercell x-ray cross-talk reduction was evaluated using Monte Carlo simulations. The detector presampling modulation transfer function (MTF) of the proposed detector was simulated to characterize the influence of cross-talk reduction on the scanner's spatial resolution.

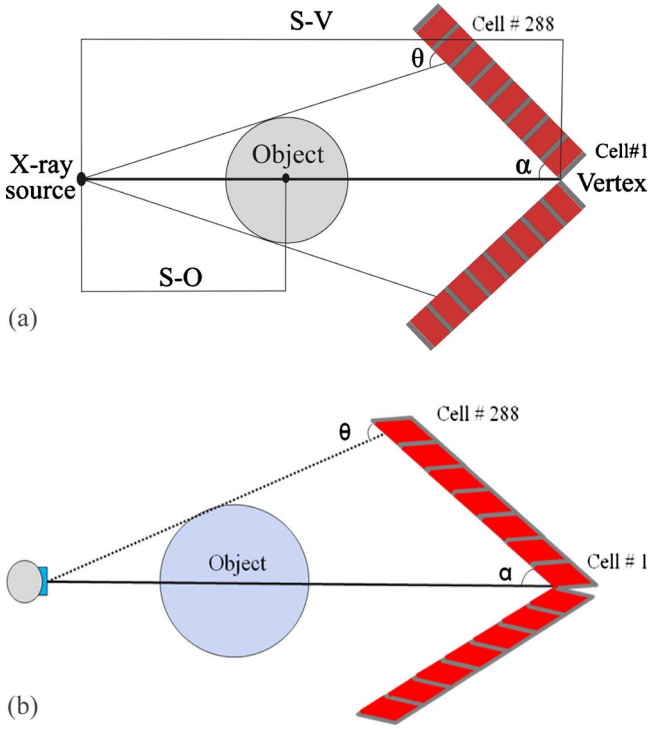

FIG. 1. Schematic diagram of the VRX CT scanner using the perpendicular cell detector design (a) and the oriented cell detector design (b).

II. MATERIALS AND METHODS

II.A. VRX CT scanner

Figure 1(a) depicts the diagram of a typical VRX CT scanner consisting of two VRX detector arms. The detector arms can rotate around a common pivotal point (vertex). Among the various VRX detector models, the dual-arm geometry is preferable because of its left-right symmetry, low magnification nonuniformity from one end of the detector to the other, and compact system design.[20] A schematic diagram of the proposed oriented cell detector design is depicted in Fig. 1(b).

The VRX CT scanner also includes an x-ray tube placed at a defined source-vertex distance (S-V). The object is placed at source-object distance (S-O). In the diagram, α is the opening half angle and θ is the incident angle of the respective cell. The diameter of the circle (object size) corresponds to the FOV of the VRX CT scanner, which depends on the opening half angle (α) and active length of the detector. The FOV of the system varies from 0.5 cm (α_{min}) to 40 cm (α_{max}).

II.B. Intercell x-ray cross-talk

Intercell x-ray cross-talk has significant impact on the VRX detector performance because of the angulation of the

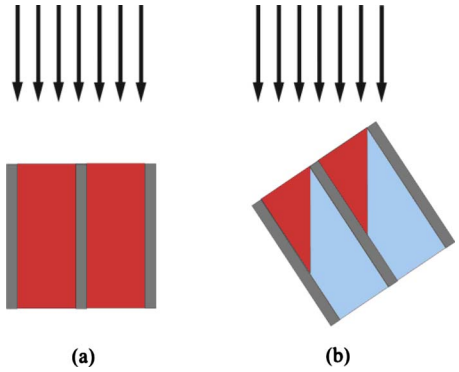

FIG. 2. The effective volume (dark area) of cells in the perpendicular detector design for (a) x-ray beam incident angle of 90° and (b) acute incident angle.

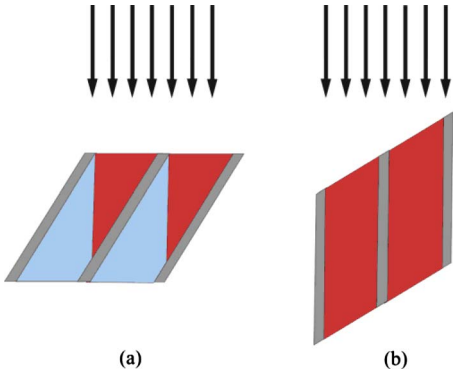

FIG. 3. The effective volume (dark area) of cells in the oriented detector design for (a) x-ray beam incident angle of 90° and (b) acute incident angle.

detector. Since in conventional CT scanners the detector is orthogonal to the incident x-ray beam, the cross-talk makes the LSF of the detector symmetrical. In the VRX detector, where the angle between the detector and the incident x-ray beam changes, the LSF of the detector is no longer symmetrical.[7] As the opening half angle decreases, the LSF of the detector is expected to be less symmetrical. In addition, since the angle between the incident x-ray beam and the detector surface varies at different FOVs in VRX CT scanners, intercell x-ray cross-talk is more severe in comparison with conventional CT scanners. In this study, the intercell x-ray cross-talk refers to the percentage of the deposited energy in the cell under study from x-ray photons penetrating through cell separators from the neighboring cells. The energy of photons, incident angle, thickness, and x-ray attenuation coefficient of cell separators are the main factors that determine the intercell x-ray cross-talk.

To evaluate intercell cross-talk, the energy deposited in a detector cell by x rays must be determined in two cases. First, there is no x-ray penetration between detector cells in the case where cell separators have infinite x-ray attenuation. This energy is called E_0 and represents the ideal case when there is no intercell x-ray cross-talk. Second, the cell separators have a given x-ray attenuation corresponding to a certain thickness of the attenuator and the deposited energy is E_p. Then, intercell x-ray cross-talk is given by[16]

$$\mathrm{IC} = 100 \times (E_p - E_0)/E_0. \quad (1)$$

Equation (1) is a benchmark to evaluate x-ray penetration between cells in the VRX detector. By simulating the energy deposited in a detector cell with ideal and actual separators, intercell x-ray cross-talk can be characterized.

II.C. Cell arrangement in the VRX detector

When the opening half angle (α) or FOV is maximum in the VRX detector, the incident x-ray beam is almost orthogonal to the detector cells (e.g., cell 144, middle detector cell). In this situation, because the incident x-ray beam is parallel to the cell separators, the intercell x-ray cross-talk is expected to be small even if the x-ray energy is high [Fig. 2(a)]. As the opening half angle or FOV in the VRX detector decreases, the x-ray incident angle (θ) with the detector will also decrease and the x-ray photons are more likely to penetrate through the cell separators [Fig. 2(b)]. Hence, intercell x-ray cross-talk is expected to increase with respect to the incident angle.

When the incident angle is almost 90° for a cell under study (e.g., cell 144), the scintillation crystal is directly exposed to x-ray photons (dark area in Fig. 2). In the VRX detector, as the incident angle decreases, the volume in the scintillation crystal that is directed toward primary photons decreases. As a result, the effective volume in the scintillation crystal decreases.

II.D. Oriented cell detector: A novel approach for VRX detector configuration

The proposed concept consists of decreasing the intercell x-ray cross-talk in the VRX detector by orientating the detector cells toward the opening end of the detector to minimize the intercell x-ray cross-talk. To fulfill this aim, the intercell x-ray cross-talk of the VRX detector should be measured for all FOVs. Thereafter, according to the FOVs in which maximum intercell x-ray cross-talk occurs, the optimum cell orientation angle can be calculated. The magnitude of intercell x-ray cross-talk in the oriented cell detector is quantified through simulations under the same conditions for both detector designs (the same x-ray tube voltage and source-detector arrangement).

Under this condition, when the incident angle is 90°, the cell separators are no longer parallel to the x-ray beam [Fig. 3(a)]. The maximum intercell x-ray cross-talk occurs at maximum FOV (or opening half angle). As the opening half angle decreases, the cell separators become parallel to the incident x-ray beam [Fig. 3(b)] and as such the intercell x-ray cross-talk will decrease as the opening half angle (or FOV) decreases.

II.E. VRX CT scanner model

To evaluate intercell x-ray cross-talk in the VRX detector, we used a geometrical model based on the VRX CT scanner designed and built by Melnyk and DiBianca.[16] Monte Carlo simulation techniques were used to estimate intercell x-ray

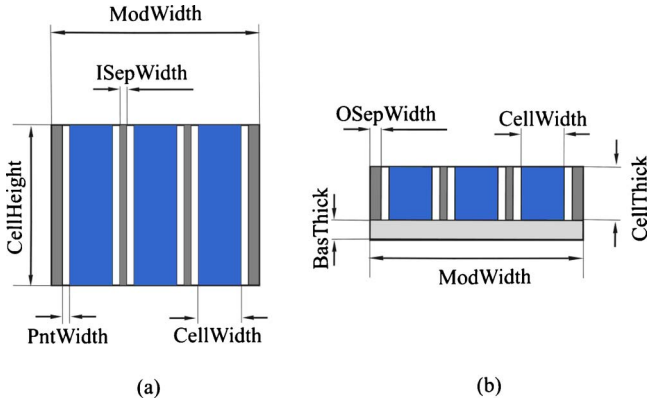

FIG. 4. Schematic representation of the perpendicular cell VRX detector model: (a) Front view of the detector and (b) upper view of the detector (Ref. 16).

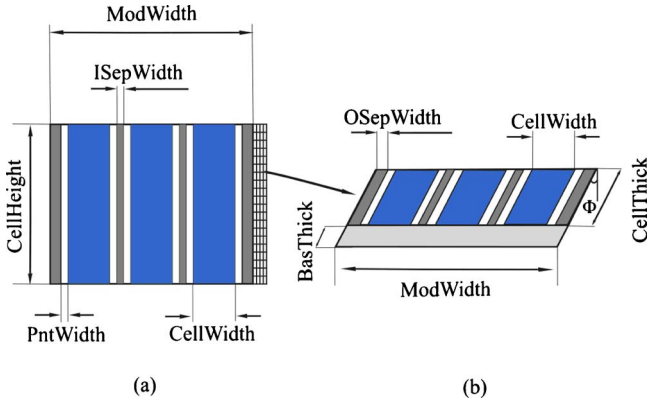

FIG. 5. Schematic representation of the oriented cell detector model: (a) Front view of detector and (b) upper view of detector.

cross-talk in the VRX detector and to predict the performance of the newly proposed design using oriented cells. Figure 4 depicts the main components of the VRX detector. Cadmium tungstate scintillator ($CdWO_4$) is used as detector for this system with a width of *Cellwidth*, height of *CellHeight*, and thickness of *CellThick*. One detector module includes 24 cells separated by inner cell separators of width *ISepWidth*. On the edge of each module there are two outer separators of width *OSepWidth*. Both types of separators are made of lead (Pb). In the actual detector, there is a reflective paint between the cells and the separators. In the simulation model, a gap having a width of *PntWidth* is considered instead of the reflective paint. Behind the cells, there is a layer of aluminum oxide (Al_2O_3) with a thickness of *BasThick*.

The actual VRX CT scanner has two detector arms where each arm consists of 12 modules with 288 discrete cells. In this work, only one detector arm with 12 modules is used. Table I summarizes the parameters of the VRX detector model. Following simulation of intercell x-ray cross-talk in the considered VRX detector model (Fig. 4) and calculation of the optimum cell orientation angle (Φ), Monte Carlo simulations were repeated for oriented cell detector module (Fig. 5). In the oriented cell detector, all design parameters and dimensions are similar to the actual detector, the only difference being the orientation of the detector cells.

Our geometrical model is based on a typical VRX CT scanner (Fig. 1). The source-vertex distance is 150 cm, whereas the source-object distance is constant for all FOVs and is equal to 125.9 cm. At the maximum FOV, the incident angle for the middle arm cell is 90°, whereas the active length of the detector is 239.07 mm.[16]

TABLE I. Design parameters of the VRX CT scanner model (Ref. 16).

Parameter	Dimension (mm)
Cell width, *CellWidth*	0.79
Cell height, *CellHeight*	20.14
Cell thickness, *CellThick*	3.00
Inner separator width, *ISepWidth*	0.10
Outer separator width, *OSepWidth*	0.18
Reflective paint width, *PntWidth*	0.05
Module base thickness, *BasThick*	1.02
Module width, *ModWidth*	24.02

II.F. X-ray source model

In the proposed model, we used a polychromatic x-ray beam for the simulation of intercell x-ray cross-talk in the VRX detector. The *Spektr* tool was used for the generation of the x-ray beam spectrum.[21] Spektr is a computational tool for x-ray analysis based on the method of interpolating polynomials, called TASMIP.[22] To generate the beam spectrum, an intrinsic aluminum filtration of 1.2 mm was used. The tube voltage in the VRX CT is not constant and varies as a function of the FOV to produce a constant x-ray penetration fraction at each FOV. The x-ray penetration fraction of a tube voltage of 120 kVp and a cylindrical water phantom of 40 cm was the reference for obtaining tube voltages at other FOVs. The obtained fraction (0.03%) was used for the calculation of tube voltages at other FOVs. For each FOV, a cylindrical water phantom having the diameter of the corresponding FOV was used and the tube voltage altered until the same fraction of 0.03% at each FOV was reached. This procedure allowed the derivation of tube voltages for the simulation study actually varying nonlinearly from 10 kVp at a FOV of 1 cm to 120 kVp at a FOV of 40 cm (Fig. 6).

II.G. Monte Carlo simulations

A previous study reported on the assessment of the intercell x-ray cross-talk in the VRX detector as a function of the FOV size using Monte Carlo simulations.[16] The GATE package[23] was used to quantify the intercell x-ray cross-talk in the VRX detector. GATE is a dedicated Monte Carlo simulation package for modeling medical imaging systems. After accurate modeling of cross-talk in GATE, the oriented cell detector geometry was implemented to assess its potential in reducing the intercell x-ray cross-talk. The optimum cell orientation angle was calculated according to the peak of the intercell x-ray cross-talk and its corresponding x-ray incident angle. The optimum orientation angle was calculated such

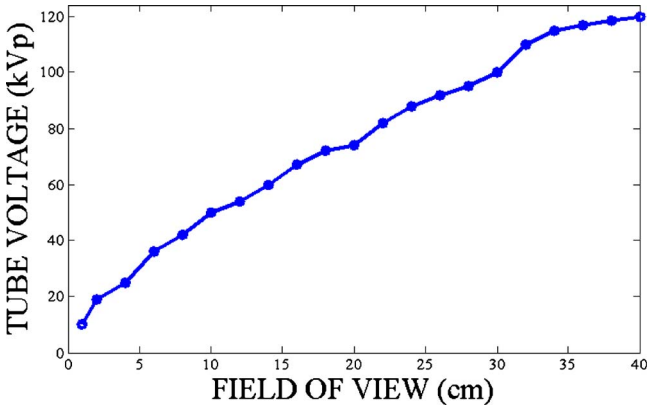

FIG. 6. Plot of the x-ray tube voltage versus the FOV of the VRX CT scanner.

that the detector cells are almost orthogonal to the incident x-ray beam at the FOV corresponding to the peak of x-ray cross-talk. It should be noted that the optimum orientation angle was obtained for the middle detector cell (cell 144) and was then applied to all detector cells. The spatial resolution nonuniformity resulting from x-ray cross-talk is expected to be reduced since detector cells are oriented according to the optimum orientation angle of the middle detector cell.

The program was run twice for each FOV to compute the intercell x-ray cross-talk. First, the deposited energy in the cell under study (cell 144) was estimated when the cell separators have ideally high x-ray attenuation. This energy corresponds to E_0 in Eq. (1). The same simulation was then repeated with the lead cell separators in place to calculate E_p.

II.H. Detector presampling MTF

The MTF is deemed to be a standard measure of the spatial resolution for imaging systems. It gives an account of the transfer of sinusoidal inputs through the system.[19] The detector presampling MTF is considered as one of the most relevant measures of the spatial resolution for digital imaging systems.[24] In detector presampling MTF, only detector aperture and blurring in the detection medium are incorporated and as such this MTF describes the inherent resolution of one cell in a discrete detector, while the influence of other factors, such as focal spot, magnification, sampling, or reconstruction, are overlooked. The detector presampling MTF is an ideal measure for performance comparison of the two detector designs investigated in this work.

Experimental characterization of detector presampling MTF is usually done through measurement of the corresponding LSF or edge spread function (ESF). The LSF and ESF are, respectively, defined as the radiation intensity distribution in the images of perfectly attenuating line and edge objects of unit intensity.[19] For 1D discrete detectors, the detector presampling LSF is measured by the moving slit/wire method in which the image of a slit or wire is acquired by one detector cell with adequate samples. In this method, the object is shifted over the detector cell under study and, at each position, one sample of the LSF is obtained.[17,25,26] Once the detector presampling LSF is measured, the corresponding MTF can be computed as

$$\mathrm{MTF}(f) = c\left|F\{\mathrm{LSF}(x)\}\right|, \tag{2}$$

where $F\{\ \}$ represents the Fourier transform, c is a normalization constant, and x and f are the spatial and frequency coordinates, respectively.

Quantification of detector presampling MTF is performed by evaluating the corresponding LSF. By modeling the LSF of the two detector designs, the corresponding detector presampling MTF can be calculated.

II.I. Modeling of detector presampling MTF

The detector presampling MTF of the two detector models (oriented and perpendicular cells) was estimated under similar simulation conditions to assess the impact of x-ray cross-talk reduction on the system spatial resolution. Since the two VRX detector models were designed using 1D discrete arrays, modeling of the detector presampling MTF was done by "moving" a perfectly zero-thickness pencil x-ray beam using a very small step along the detector arrays and recording the energy deposited in the cell under study as a function of the beam position. Since GATE provides the capability to use a perfect pencil beam, there was no need to simulate the slit. The magnitude of the deposited energy at each step represents the detector presampling LSF, from which the corresponding MTF was computed using Eq. (2).

The detector presampling MTF of the two detector models was obtained as a function of the FOV. For each FOV, the detector models with cell separators from lead were used for the simulation of the MTF. A polychromatic x-ray point source was used to create a pencil beam. The source spectrum was similar to the setup used for measurement of the intercell x-ray cross-talk. There is a slight spatial resolution nonuniformity along the VRX detector because of its angulation and different cell-source distances. For this reason, the detector presampling MTF was measured for cell 144 (middle detector cell) to present the average MTF of the detector cells.

The number of samples in each simulated LSF was 600. The x-ray beam was therefore shifted 600 times along the detector array over the cell under study with very small steps. This procedure was facilitated by the GATE code's ability to shift the source during simulation. The amount of shifting (LSF sampling distance) was equal to 1/20 of the projected cell width on the object plane. Following computation of the detector presampling MTF, the spatial frequency at MTF=0.1 was used as estimate of the spatial resolution of the detector model for each FOV.

III. RESULTS

Figure 7 shows the validation of the GATE simulation model used in this work for lead separator through comparison with the results published by Melnyk and DiBianca.[16] The maximum intercell x-ray cross-talk occurred between FOVs of 34 and 38 cm (>12%). Although the incident angle

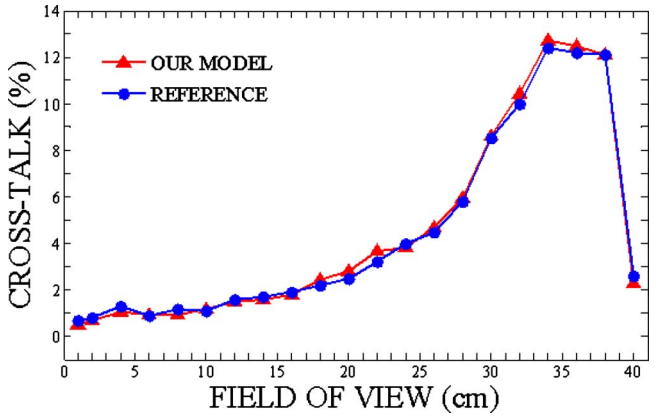

FIG. 7. Plot of the intercell x-ray cross-talk for the VRX detector comparing Monte Carlo simulation results obtained using GATE to those reported by Melnyk and DiBianca (Ref. 16) used as a reference for comparison.

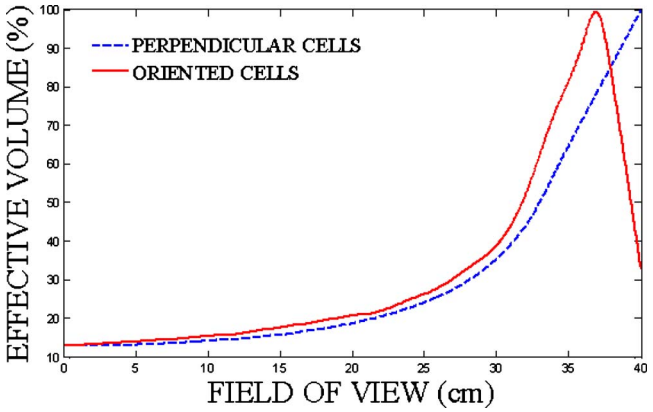

FIG. 9. Plot of the effective cell volume for perpendicular and oriented cell detector models versus the FOV of the VRX CT scanner.

was very small at smaller FOVs, intercell x-ray cross-talk was relatively low (<3%) because of low x-ray tube voltage. The assessment of intercell x-ray cross-talk versus the FOV and incident angles in which the maximum cross-talk occurred revealed an optimum orientation angle of the detector cells (Φ) of 28°. Since the average incident angle for FOVs of 38–34 cm (peak cross-talk) was almost 62°, the detector cells will be placed approximately orthogonal to the incident x-ray beam at these FOVs when the orientation angle is equal to 28°.

Figure 8 shows the intercell x-ray cross-talk for the oriented cell detector. It should be noted that the cross-talk for both perpendicular and oriented cell detectors were obtained under the same simulation setup, while the tube voltage changed from 10 kVp (at 1 cm FOV) to 120 kVp (at 40 cm FOV).

In the oriented cell detector, the maximum intercell x-ray cross-talk occurred at a FOV of 40 cm with a corresponding maximum tube voltage of 120 kVp. As the FOV or opening half angle (α) decreases, the cells and separators become parallel to the incident x-ray beam. Hence, the intercell x-ray cross-talk decreases greatly at FOVs from 24 to 38 cm. In the perpendicular cell detector, the spatial resolution of the system is considerably limited by high intercell x-ray cross-talk at FOVs of 24–38 cm. By using the oriented cell detector, the spatial resolution of the system could be improved for a wide range of FOVs.

As discussed earlier, when the opening half angle of the VRX detector decreases, the effective volume (directly exposed to the x-ray beam) of the detector cells decreases. Figure 9 shows the effective volume of the cell under study for the perpendicular and oriented cells' arrangement of the VRX detector as a function of the FOV.

When the cells are oriented, the maximum effective volume of the cell under study was placed at FOVs of 32–38 cm. The intercell x-ray cross-talk decreases significantly at FOVs within 32–38 cm with a high cross-talk at a FOV of 40 cm. The deposited energy in the cell under study for the actual VRX detector model (perpendicular cells) and for the oriented cell detector was equal under similar simulation conditions (Fig. 10). Therefore, orienting the detector cells had no effect on the efficiency of the detector.

Figure 11 depicts the detector presampling MTF of the oriented and perpendicular cell models. The spatial resolution was calculated for cell 144 (middle detector cell) keeping in mind that the spatial resolution for other cells was almost similar. The detector presampling MTF of the system

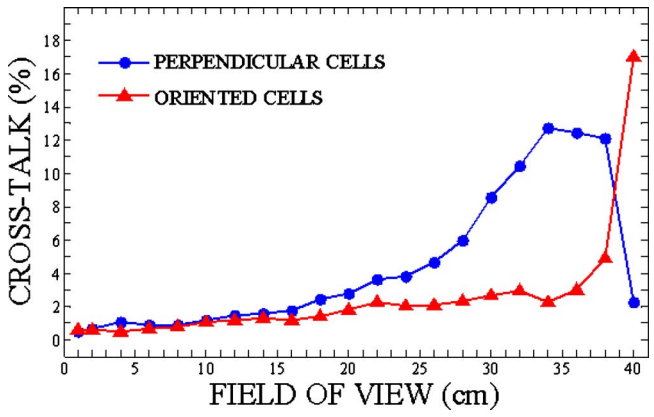

FIG. 8. Comparison of the intercell x-ray cross-talk obtained by Monte Carlo simulations of the perpendicular and oriented cell detector designs.

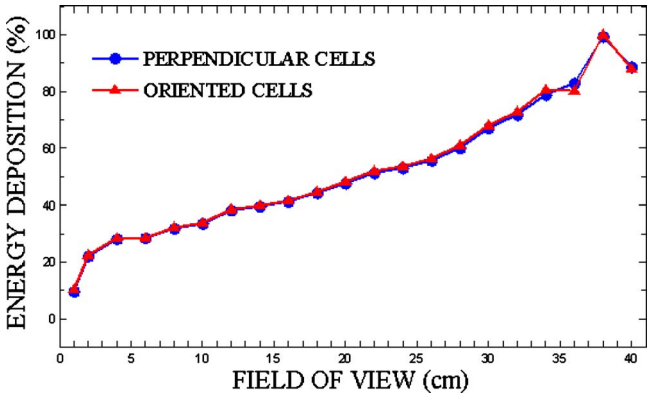

FIG. 10. Plot of the deposited energy in the cell under study for the perpendicular and oriented cell detector models.

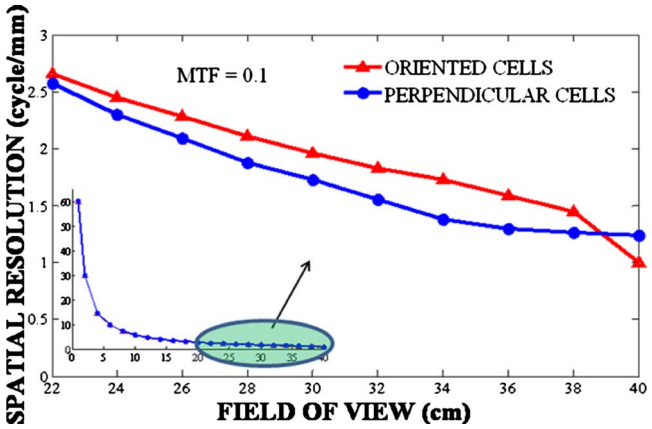

FIG. 11. Plot of the detector presampling MTF (MTF=0.1) of the perpendicular and oriented cell detector models for the middle detector cell (cell 144) versus the FOV.

varied from about 1 cycle/mm at a FOV of 40 cm to more than 60 cycles/mm at a FOV of 1 cm. Since the reduction in the intercell x-ray cross-talk appeared mostly in FOVs of 40–22 cm, this span was magnified in Fig. 11.

IV. DISCUSSION

Intercell x-ray cross-talk is an important issue in the VRX CT detector because of its profound impact on the resulting spatial resolution of the scanner. Through angulation of the detector, the angle between the incident x-ray beam and the detector face (θ) varies at different FOVs, which results in a more severe intercell x-ray cross-talk in the VRX detectors. The intercell x-ray cross-talk substantially affects the spatial resolution of the system.[4,16] In addition, for a given FOV, the incident angle and, consequently, x-ray cross-talk differ from one end of the detector to the other, which causes spatial resolution nonuniformity along the detector.

The intercell x-ray cross-talk for this specific VRX detector design was critical at FOVs from 24 to 38 cm. The x-ray tube voltage decreases gradually from 120 to 10 kVp as a function of the FOV. At FOVs of 24–38 cm, the tube voltage is relatively high and the cell separators are at an acute angle with respect to the incident x-ray beam. Consequently, the maximum cross-talk occurred at these FOVs. Although the incident angle is very small at small FOVs, the low x-ray tube voltage caused a substantial decrease in the x-ray cross-talk. Similarly, in spite of the high x-ray tube voltage at a FOV of 40 cm, the incident angle was almost 90°, resulting in a reduction in the x-ray cross-talk. The high intercell x-ray cross-talk at FOVs of 24–38 cm causes a considerable degradation of the spatial resolution, which produces an asymmetric system's LSF.

For variable x-ray tube voltage, the optimum cell's orientation angle (Φ) was 28°. Any change in the tube voltage leads to different optimum cell's orientation angles for this system. In addition to the high intercell x-ray cross-talk at a FOV of 40 cm, the dependency of the optimum cell's orientation angle on the tube voltage and scanner configuration (source-detector distance) accounts for the main weakness of the oriented cell detector design. Assuming that the tube voltage is fixed at all opening half angles, the x-ray cross-talk tends to increase as the FOV decreases. Therefore, a FOV of 40 cm produces the minimum x-ray cross-talk because the incident angle is almost 90°. Conversely, a FOV of 1 cm produces the largest x-ray cross-talk. In this case, the optimum cell's orientation angle is 45°. Such detector modules (with cells orientation angle of 45°) are suitable for four-arm VRX CT scanners.[10] In such scanners, the FOV has a small range of variation and as such the x-ray tube voltage is almost fixed despite the variable incident angle of detector cells. The oriented cell detector design with an angle of 45° would significantly reduce the intercell x-ray cross-talk in the four-arm VRX CT scanner.

In the oriented cell detector, the x-ray cross-talk is critical only at a FOV of 40 cm. The intercell x-ray cross-talk increased from 2% to 17% for this FOV size. The high x-ray cross-talk at a FOV of 40 cm is the sole disadvantage of the oriented cell detector. At this FOV, the cell separators are no longer parallel to the incident x-ray beam and the tube voltage is at its maximum. Both factors increased considerably the x-ray cross-talk. By reducing the FOV, the cell separators are placed almost parallel to the x-ray beam and as such the x-ray cross-talk decreased significantly. The intercell x-ray cross-talk decreased from 12% to less than 5% for FOVs of 38–24 cm, respectively. At small FOVs, the incident angle plays a minor role because the tube voltage was sufficiently low to produce negligible x-ray cross-talk. For FOVs larger than 40 cm, there is a steep slope in cross-talk for both perpendicular and oriented cell detectors (Fig. 8) because the change in the opening half angle was comparably high between FOVs of 38 and 40 cm. In the oriented cell detector, this sharp slope was negative and a FOV of 40 cm was abandoned to provide low intercell x-ray cross-talk for other FOVs.

The detector presampling MTF includes only detector aperture and blurring in the detection medium. Hence, this MTF describes the inherent spatial resolution of one cell in a discrete detector reflecting intercell x-ray cross-talk as the dominant degrading factor. Because intercell x-ray cross-talk was very low at small FOVs (below 16 cm) for both oriented and perpendicular cell models, the detector presampling MTF of these detector models were almost the same for small FOVs. At large FOVs, the detector presampling MTF of the oriented cell detector model increases up to 0.5 cycle/mm because of the reduction in the intercell x-ray cross-talk.

According to the simulation results of Melnyk and DiBianca,[16] using tungstate cell separators (instead of lead) could decrease the intercell x-ray cross-talk by up to 20%. Using tungstate cell separators in the oriented cell detector would decrease even more the x-ray cross-talk. By increasing the thickness of cell separators, the intercell x-ray cross-talk can be further reduced but at the expense of considerably decreasing the efficiency of the detector. The reduction in the x-ray cross-talk could be achieved by the oriented cell detector without affecting the detector efficiency at various FOVs.

The oriented cell detector can provide higher spatial and

contrast resolution in VRX CT scanners. Besides, the spatial resolution nonuniformity along the detector length owing to the effect of intercell x-ray cross-talk would be reduced. The same design can be applied in flat-panel and cone-beam VRX CT scanners to achieve a higher spatial resolution. In multislice VRX CT scanner, each detector row can be tilted toward the center of rotation to provide lower interslice x-ray cross-talk in addition to the detector cell orientation.

This study demonstrates that the oriented cell detector can considerably reduce intercell x-ray cross-talk in the VRX CT scanner. The possibility to reduce the relatively high intercell x-ray cross-talk at a FOV of 40 cm is a subject for further research. The development of a novel method to minimize intercell x-ray cross-talk at a FOV of 40 cm would make the oriented cell detector design an ideal option for VRX CT scanners.

V. CONCLUSION

A novel detector design based on the oriented cells was proposed for the VRX CT scanner where the cells are oriented toward the opening end of detectors to reduce the intercell x-ray cross-talk. The performance of the proposed design was evaluated using GATE Monte Carlo simulations. An optimum cell orientation angle of 28° was obtained for one specific VRX CT scanner design. In the oriented cell detector, the intercell x-ray cross-talk decreased by up to 8% for FOVs varying from 24 to 38 cm. The intercell x-ray cross-talk in the oriented cell detector was below 5%, thus resulting in a higher spatial resolution for all FOVs, except for a FOV of 40 cm. The deposited energy in the oriented cell detector had no significant difference in comparison with the perpendicular detector design. As a result, the efficiency of the detector remained unchanged in the new design. It was concluded that the oriented cell detector could substantially reduce the intercell x-ray cross-talk in the VRX CT scanner. The same concept can be applied to multislice and flat-panel VRX CT detectors to improve their spatial resolution.

ACKNOWLEDGMENTS

This work was supported by the Research Department of Shahid Beheshti University, the Swiss National Science Foundation under Grant No. 31003A-125246, and the Geneva Cancer League.

[a]Author to whom correspondence should be addressed. Electronic mail: a_kamali@sbu.ac.ir; Telephone: +98 21 29903178; Fax: +98 21 22431780.

[1]J. Beutel, H. L. Kundel, and R. L. van Metter, editors, *Physics and Psychophysics. 1*, Handbook of Medical Imaging (SPIE, Bellingham, 2000).
[2]G. Wang, S. Zhao, H. Yu, C. Miller, P. Abbas, B. Gantz, S. Lee, and J. Rubinstein, "Design, analysis and simulation for development of the first clinical micro-CT scanner," Acad. Radiol. **12**, 511–525 (2005).
[3]A. Sasov and D. van Dyck, "Desktop x-ray microscopy and microtomography," J. Microsc. **191**, 151–158 (1998).
[4]F. A. DiBianca, V. Gupta, and H. D. Zeman, "A variable resolution x-ray detector for computed tomography: I. Theoretical basis and experimental verification," Med. Phys. **27**(8), 1865–1874 (2000).
[5]F. A. DiBianca, P. Zou, L. M. Jordan, J. S. Laughter, H. D. Zeman, and J. Sebes, "A variable resolution x-ray detector for computed tomography: II. Imaging theory and performance," Med. Phys. **27**(8), 1875–1880 (2000).
[6]F. A. DiBianca, R. Melnyk, A. Sambari, L. M. Jordan, J. S. Laughter, and P. Zou, "A solid-state VRX CT detector," Proc. SPIE **3977**, 205–210 (2000).
[7]R. Melnyk and F. A. DiBianca, "Modeling and measurement of the detector presampling MTF of a variable resolution x-ray CT scanner," Med. Phys. **34**(3), 1062–1075 (2007).
[8]B. Dahi, G. S. Keyes, D. A. Rendon, and F. A. DiBianca, "Performance analysis of a CsI-based flat panel detector in a cone beam variable resolution x-ray system," Proc. SPIE **6510**, 65104B–8 (2007).
[9]B. Dahi, G. S. Keyes, D. A. Rendon, and F. A. DiBianca, "Analysis of axial spatial resolution in a variable resolution x-ray cone beam CT (VRX-CBCT)," Proc. SPIE **6913**, 69134Y–8 (2008).
[10]F. A. DiBianca, D. Gulabani, L. M. Jordan, S. Vangala, D. Rendon, J. S. Laughter, R. Melnyk, M. W. Gaber, and G. S. Keyes, "Four-arm variable-resolution x-ray detector for CT target imaging," Proc. SPIE **5745**, 332–339 (2005).
[11]D. A. Rendon, F. A. DiBianca, and G. S. Keyes, "Comparison of multi-arm VRX CT scanners through computer models," Proc. SPIE **6510**, 65103Y–9 (2007).
[12]L. M. Jordan, F. A. DiBianca, P. Zou, J. S. Laughter, and H. D. Zeman, "Processing of CT sinograms acquired using a VRX detector," Proc. SPIE **3977**, 570–579 (2000).
[13]A. R. Kamali Asl, H. Arabi, and S. Tamhidi, "Optimization of magnification in a VRX CT scanner," IFMBE Proc. **25**(2), 266–269 (2009).
[14]L. M. Jordan, F. A. DiBianca, R. Melnyk, A. Choudhary, H. Shukla, J. Laughter, and M. W. Gaber, "Determination of calibration parameters of a VRX CT system using an 'Amoeba' algorithm," J. X-Ray Sci. Technol. **12**, 281–293 (2004).
[15]H. Arabi, A. R. Kamali Asl, and S. M. Aghamiri, "The effect of focal spot size on the spatial resolution of variable resolution x-ray CT scanner," Iranian Journal of Radiation Research **8**(1), 37–43 (2010).
[16]R. Melnyk and F. A. DiBianca, "Monte Carlo study of x-ray cross talk in a variable resolution x-ray detector," Proc. SPIE **5030**, 694–701 (2003).
[17]E. Samei, N. T. Ranger, J. T. I. Dobbins, and Y. Chen, "Intercomparison of methods for image quality characterization. I. Modulation transfer function," Med. Phys. **33**, 1454–1465 (2006).
[18]E. Samei, M. J. Flynn, and D. A. Reimann, "A method for measuring the presampled MTF of digital radiographic systems using an edge test device," Med. Phys. **25**(1), 102–113 (1998).
[19]K. Rossmann, "Point spread-function, line spread-function, and modulation transfer function. Tools for the study of imaging systems," Radiology **93**, 257–272 (1969).
[20]F. A. DiBianca, R. Melnyk, C. N. Duckworth, S. Russ, L. M. Jordan, and J. S. Laughter, "Comparison of VRX CT scanners geometries," Proc. SPIE **4320**, 627–635 (2001).
[21]J. H. Siewerdsen, A. M. Waese, D. J. Moseley, S. Richard, and D. A. Jaffray, "Spektr: A computational tool for x-ray spectral analysis and imaging system optimization," Med. Phys. **31**(11), 3057–67 (2004).
[22]J. M. Boone and J. A. Seibert, "An accurate method for computer generating tungsten anode x-ray spectra from 30 to 140 kV," Med. Phys. **24**, 1661–1670 (1997).
[23]S. Jan *et al.*, "GATE: A simulation toolkit for PET and SPECT," Phys. Med. Biol. **49**(19), 4543–4561 (2004).
[24]J. T. I. Dobbins, "Effects of undersampling on the proper interpretation of modulation transfer function, noise power spectra, and noise equivalent quanta of digital imaging systems," Med. Phys. **22**, 171–181 (1995).
[25]H. Fujita, D. Y. Tsai, T. Itoh, K. Doi, J. Morishita, K. Ueda, and A. Ohtsuka, "A simple method for determining the modulation transfer function in digital radiography," IEEE Trans. Med. Imaging **11**, 34–39 (1992).
[26]J. T. I. Dobbins, D. L. Ergun, L. Rutz, D. A. Hinshaw, H. Blume, and D. C. Clark, "DQE(f) of four generations of computed radiography acquisition devices," Med. Phys. **22**, 1581–1593 (1995).